



## Superfluid turbulence: Nonthermal fixed point in an ultracold Bose gas

Boris Nowak, Dénes Sexty, and Thomas Gasenzer\*

*Institut für Theoretische Physik, Ruprecht-Karls-Universität Heidelberg, Philosophenweg 16, D-69120 Heidelberg, Germany*

*ExtreMe Matter Institute EMMI, GSI Helmholtzzentrum für Schwerionenforschung GmbH, Planckstrasse 1, D-64291 Darmstadt, Germany*

(Received 21 June 2011; published 20 July 2011)

Nonthermal fixed points of the dynamics of a dilute degenerate Bose gas are analyzed in two and three spatial dimensions. For such systems, universal power-law distributions, previously found within a nonperturbative quantum-field theoretic approach, are shown to be related to vortical dynamics and superfluid turbulence. The results imply an interpretation of the momentum scaling at the nonthermal fixed points in terms of independent vortex excitations of the superfluid. Long-wavelength acoustic excitations on the top of these are found to follow a nonthermal power law. The results shed light on fundamental aspects of superfluid turbulence and have strong potential implications for related phenomena, e.g., in early-universe inflation or quark-gluon plasma dynamics.

DOI: [10.1103/PhysRevB.84.020506](https://doi.org/10.1103/PhysRevB.84.020506)

PACS number(s): 67.85.-d, 47.27.-i, 47.70.Nd, 67.10.-j

From the formation of Bose-Einstein condensates in ultracold gases to quark-gluon plasmas produced in heavy-ion collisions, over a range of 24 orders of magnitude in temperature, nonequilibrium dynamics governs many interesting phenomena. Turbulence is an outstanding and intricate example, which can be described as an oriented stationary flow of energy or particles between different scales. This idea of an energy cascade goes back to the work of Richardson in the context of atmospheric science.<sup>1</sup> Kolmogorov, in his 1941 mathematical discussion of turbulence in an incompressible fluid, added the concept of universality and scaling.<sup>2</sup> More recently, turbulence has been studied in the context of the inflationary early universe as well as of strongly correlated matter produced in heavy-ion collisions.<sup>3-7</sup> Dynamical critical phenomena, i.e., fixed points of the evolution away from thermal equilibrium, have been proposed. They potentially affect the equilibration process by forcing the evolution to critically slow down before final thermalization. Different scaling laws were found by analyzing nonperturbative Kadanoff-Baym dynamic equations.<sup>4,5</sup> Analogous predictions for a nonrelativistic Bose gas were given in Ref. 6, proposing strong matter-wave turbulence in the regime of long-range excitations.

Superfluid turbulence, also referred to as quantum turbulence (QT), has been the subject of extensive studies in the context of helium.<sup>8</sup> In contrast to eddies in classical fluids, vorticity in a superfluid is quantized,<sup>9,10</sup> and the creation and annihilation processes of quantized vortices are distinctly different.<sup>8</sup> The observation of a Kolmogorov 5/3 law<sup>2</sup> in experiments with superfluid helium (cf. Ref. 11 for a review) received much attention.<sup>12-16</sup> In particular, the role of the normal-fluid component as compared to the superfluid component in the turbulent flow is under debate.<sup>8</sup> In the context of the kinetics of condensation and the development of long-range order in a dilute Bose gas, the role of turbulence in the superfluid and its acoustic excitations was discussed in Refs. 17 and 18—see also Ref. 19 for a recent review. A possible observation of QT in ultracold atomic gases presently poses an exciting task for experiments.<sup>20,21</sup>

A satisfactory *ab initio* mathematical description of both quantum and classical turbulence is inherently difficult due to the generically strong correlations building up within the system. Analytical results are known, however, in regimes where kinetic theory applies: In a dilute, degenerate Bose gas

the normal-fluid component can vary at the expense or gain of the superfluid part. As a consequence, the gas is compressible and so-called weak-wave-turbulence phenomena can occur. For these, scaling laws can be derived by analyzing kinetic equations.<sup>22</sup>

Recent developments presented in Refs. 4-7 allow to set up a unifying description of scaling, both in the ultraviolet quantum-Boltzmann regime and in the infrared (IR) regime of long wavelengths where perturbation theory fails. In the IR, modified scaling laws were found<sup>4</sup> by analyzing nonperturbative Kadanoff-Baym equations with respect to nonthermal stationary solutions.

Here, we study QT in two- and three-dimensional dilute Bose gases by means of simulations in the classical-wave limit of the underlying quantum-field theory. We compare the scaling exponents of the single-particle momentum distribution and their analytical predictions.<sup>6</sup> While we find excellent agreement, our results provide an interpretation of the dynamical fixed points proposed in Refs. 4 and 6 for the case of an ultracold Bose gas: The appearance of nonperturbative infrared scaling reflects the presence of independent vortices. Moreover, the power spectra of underlying compressible excitations suggest an understanding in terms of acoustic turbulence<sup>22</sup> on the top of the vorticity-bearing quasicondensate.

*Scaling laws: Analytical predictions.* Based on the concept of universality, the turbulent single-particle spectrum  $n(\mathbf{k})$  is assumed to scale as

$$n(s\mathbf{k}) = s^{-\zeta} n(\mathbf{k}), \quad (1)$$

where  $s$  is some positive real number. This scaling law is compatible with a more general scaling behavior assumed for the full two-point correlation function of the bosonic quantum field as discussed in Ref. 6.

To determine the positive exponent  $\zeta$  in the infrared, where  $n(\mathbf{k}) \sim |\mathbf{k}|^{-\zeta}$  is large, an approach beyond kinetic weak-wave-turbulence theory has been used. This is based on analyzing fixed points of Kadanoff-Baym dynamic equations derived from the two-particle irreducible (2PI) effective action or  $\Phi$  functional. While in the regime of large wave numbers the approach goes over into the kinetic description of weak wave turbulence, an effectively renormalized many-body  $T$  matrix modifies the scaling law in the IR. This is a

consequence of the resummation of a particular class of Feynman diagrams contributing to the 2PI effective action,<sup>4,6</sup> a formulation substantially beyond the low-order perturbative expansion used for the kinetic quantum Boltzmann equation. Physically, the renormalized  $T$  matrix implies a reduction of the effective interaction strength in the IR regime of strongly occupied modes.<sup>4</sup> As a consequence, single-particle occupation numbers rise, toward smaller  $k$ , in a steeper way than in the weak-turbulence regime. The IR scaling exponent for constant radial quasiparticle flow in  $d$  dimensions was predicted in Ref. 6 as

$$\zeta = \zeta_Q^{\text{IR}} = d + 2. \quad (2)$$

*Semiclassical field simulations.* A dilute superfluid Bose gas can be described, in the classical-wave limit, by the Gross-Pitaevskii equation (GPE)

$$i\partial_t\psi(\mathbf{x},t) = \left[ -\frac{\nabla^2}{2m} + g|\psi(\mathbf{x},t)|^2 \right] \psi(\mathbf{x},t). \quad (3)$$

(In our units  $\hbar = 1$ .)  $m$  is the boson mass, and  $g$  quantifies the interaction strength. We consider a gas in a box of size  $L^d$ ,  $d = 2, 3$ , with periodic boundary conditions. Diluteness implies that  $a \ll l$ , the interparticle spacing  $l = \bar{n}^{-1/d}$  being determined by the mean density  $\bar{n} = N/L^d$ . The initial values for the real and imaginary parts of the field  $\psi(\mathbf{k}, 0)$  were randomly chosen from a Gaussian distribution with width  $1/2$ , centered at approximately  $\sqrt{n(\mathbf{k}, 0)} \exp\{i\phi(\mathbf{k}, 0)\}$ , where  $n(\mathbf{k}, t) = \langle \psi^\dagger(\mathbf{k}, t)\psi(\mathbf{k}, t) \rangle$  is the occupation number at time  $t$  and  $\phi(\mathbf{k}, 0)$  is a random-phase angle. Correlation functions, including  $n(\mathbf{k}, t)$ , were obtained by averaging over many trajectories. We have simulated the time evolution on a grid with side length  $L = N_s a_s$ , lattice spacing  $a_s$  in  $d = 2, 3$ . To induce transport from small to large wave numbers, only a few modes near  $\mathbf{k} = 0$  were chosen to be occupied at the initial time with  $n(\mathbf{k}, 0) \gg 1$ . Such an initial state can be prepared, e.g., by Bragg scattering of photons from a Bose-Einstein condensate. During the evolution to a different equilibrium state, energy is transported to modes with higher wave number, and, given appropriate interaction strength, one observes quasistationary momentum distributions to develop prior to final thermalization.

During the intermediate stage of the equilibration quantized vortices appear. To exhibit the vortical flow we use the Madelung representation  $\psi(\mathbf{x}, t) = \sqrt{n(\mathbf{x}, t)} \exp\{i\phi(\mathbf{x}, t)\}$  of the field in terms of the density  $n(\mathbf{x}, t)$  and a phase angle  $\phi(\mathbf{x}, t)$ . This allows to express the particle current  $\mathbf{j} = i(\psi^* \nabla \psi - \psi \nabla \psi^*)/2 = n\mathbf{v}$  in terms of the velocity field  $\mathbf{v} = \nabla\phi$ .

In Fig. 1 we show the phase angle  $\phi(\mathbf{x}, t)$  during a single run in  $d = 2$  dimensions, while in Fig. 2 the evolution in  $d = 3$  is illustrated by the near-zero-density points. Many singly quantized vortex-antivortex pairs (vortex rings) are formed once the initial coherent wave has developed to form shock-wave-like fronts. During the later evolution, the pairs mutually annihilate at a substantially decreasing rate. After the last pair has vanished, the gas thermalizes. In  $d = 3$ , decreasingly tangled vortex lines are observed during the near-stationary evolution. The initial conditions lead to a dense chaotic tangle, as studied also in Refs. 18 and 19.

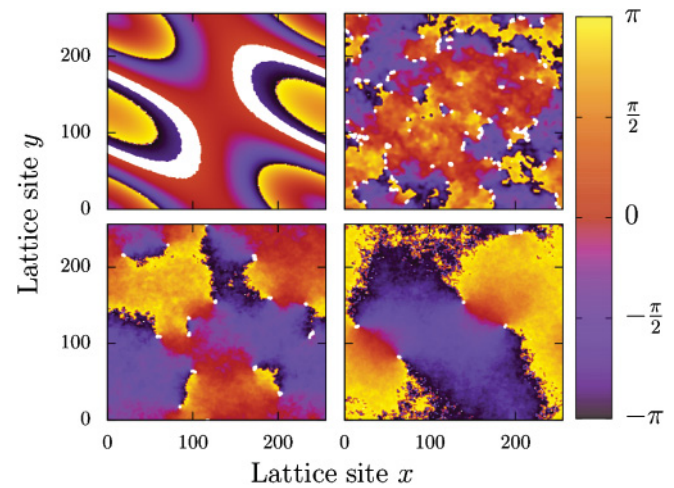


FIG. 1. (Color online) Phase angle  $\phi(\mathbf{x}, t)$  (color scale) at four times during a single run of the simulations in  $d = 2$ . The white spots mark vortex cores where the density falls below 5% of the mean density  $\bar{n}$ . Parameters are as follows:  $\bar{g} = 2mga_s^{2-d} = 3 \times 10^{-5}$ ,  $N = 10^8$ ,  $N_s = 256$ , and  $\bar{t} = t/(2ma_s^2)$ . Shown times are as follows: (1)  $\bar{t} = 26$  (top left-hand side): Ordered phase shortly after initial preparation. (2)  $\bar{t} = 820$  (top right-hand side): After creation of vortex-antivortex pairs. (3)  $\bar{t} = 6550$  (bottom left-hand side): Critical slowing down. (4)  $\bar{t} = 10^5$  (bottom right-hand side): Low density of vortex pairs before final thermalization.

Power-law behavior is found in the momentum distributions of particles and energy, as we discuss in the following. Figure 3 shows the distribution of occupation numbers  $n(k) = \int d\Omega_d n(\mathbf{k})$  over the radial momentum  $k = |\mathbf{k}|$ , for the four snapshots of the two-dimensional system depicted in Fig. 1,

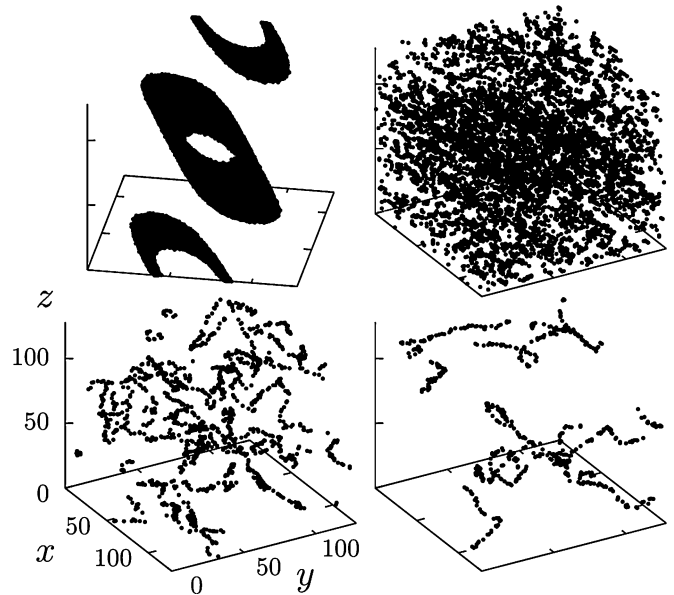


FIG. 2. Snapshots of a single run of the evolution in  $d = 3$  dimensions. The points show where the density falls below 5% of the mean density  $\bar{n}$ . Parameters are as follows:  $\bar{g} = 8 \times 10^{-4}$ ,  $N = 10^9$ ,  $N_s = 128$ . (1)  $\bar{t} = 0$  (top left-hand side). (2)  $\bar{t} = 103$  (top right-hand side). (3)  $\bar{t} = 410$  (bottom left-hand side). (4)  $\bar{t} = 1640$  (bottom right-hand side).

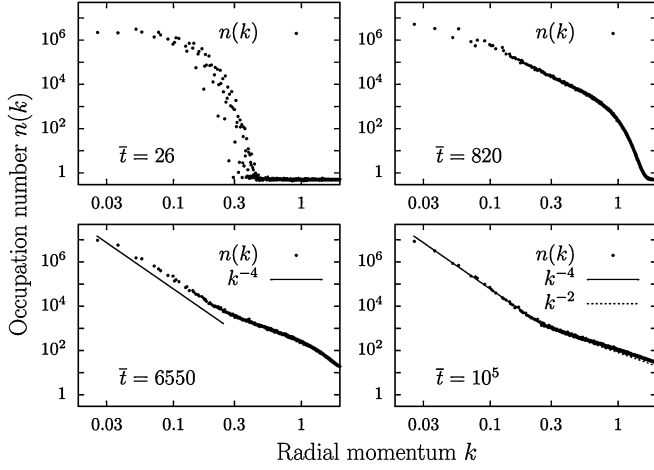


FIG. 3. Single-particle mode occupation numbers as functions of the radial momentum  $k = [\sum_{i=1}^d 4 \sin^2(k_i/2)]^{1/2}$ ,  $\mathbf{k} = 2\pi\mathbf{n}/N_s$ ,  $\mathbf{n} = (n_1, \dots, n_d)$ ,  $n_i = -N_s/2, \dots, N_s/2$ , for the four different times of the run in  $d = 2$  dimensions shown in Fig. 1. Note the double-logarithmic scale. An early development of a scaling  $n(k) \sim k^{-4}$  is followed by a bimodal scaling with  $n(k) \sim k^{-2}$  at larger wave numbers.

on a double-logarithmic scale. ( $d\Omega_d$  denotes the angular differential.) During the initial evolution the mode occupations gradually spread to larger wave numbers. As soon as vortex-antivortex pairs appear, a power-law regime  $n(k) = k^{-\zeta}$  is observed. During the final stage of the vortex-bearing phase two distinct power laws develop, which are found to be in excellent agreement with the analytical prediction of Ref. 6. While in the ultraviolet the exponent  $\zeta^{\text{UV}} = d = 2$  exhibits weak wave turbulence, in the infrared the exponent confirms the result  $\zeta = d + 2 = 4$  [see Eq. (2)], corroborating results for a relativistic model in Ref. 4. Note that in  $d = 2$ , the weak-turbulence exponent  $\zeta^{\text{UV}} = 2$  is identical to that in thermal equilibrium in the Rayleigh-Jeans regime  $n(k) \sim T/\omega \sim T/k^2$ .<sup>22</sup> The momentum distributions during this final phase are shown again, for  $d = 2$  and  $d = 3$ , in Figs. 4 and 5 (filled black circles), respectively, confirming the analytical prediction of Eq. (2) also for  $d = 3$ . The scaling  $n(k) \sim k^{-2}$  in the ultraviolet reflects that the corresponding modes are already thermalized. We remark that, for weaker interaction strengths, the weak-wave-turbulence scaling with  $\zeta^{\text{UV}} = d = 3$  is also seen, at intermediate times.

To understand these findings in the context of QT, we analyze kinetic-energy spectra as in Ref. 12. The total kinetic energy  $E_{\text{kin}} = \int d^d x \langle |\nabla\psi(\mathbf{x}, t)|^2 \rangle / 2$  can be split,  $E_{\text{kin}} = E_v + E_q$ , into a “classical” part  $E_v = \int d^d x \langle |\sqrt{n}\mathbf{v}|^2 \rangle / 2$  and a “quantum-pressure” component  $E_q = \int d^d x \langle |\nabla\sqrt{n}|^2 \rangle / 2$ . The radial energy spectra for these fractions involve the Fourier transform of the generalized velocities  $\mathbf{w}_v = \sqrt{n}\mathbf{v}$  and  $\mathbf{w}_q = \nabla\sqrt{n}$ ,

$$E_\delta(k) = \frac{1}{2} \int k^{d-1} d\Omega_d \langle |\mathbf{w}_\delta(\mathbf{k})|^2 \rangle, \quad \delta = v, q. \quad (4)$$

Note that the superfluid velocity  $\mathbf{v} = \nabla\phi$  of a single vortex diverges as  $1/r$  with the distance  $r$  from the vortex core. Hence, the Fourier transform of  $\mathbf{v}$  is ill defined and requires regularization of  $|\mathbf{v}(\mathbf{x})|$  in the vicinity of the core. In  $\mathbf{w}_v$ , this

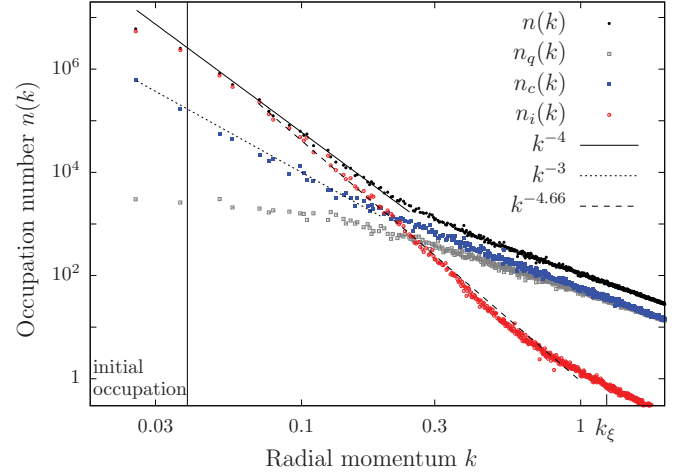


FIG. 4. (Color online) Single-particle occupation numbers of different fractions of the system, at time  $\bar{t} = 10^5$  of the  $d = 2$  run shown in Fig. 3. The black points are the same as those shown in the lower right-hand panel of Fig. 3. Colors distinguish the fractions  $n_i$  (red circles), i.e., the divergence-free part of the flow field  $\mathbf{w}_v = \sqrt{n}\mathbf{v}$ ,  $n_c$  (filled blue squares), i.e., the solenoidal part of  $\mathbf{w}_v$ , and the quantum-pressure part  $n_q$  (open gray squares).  $k_\xi = 2\pi/\xi$ , where  $\xi = 1/\sqrt{2mgn}$  is the healing length.

is naturally achieved by the factor  $\sqrt{n}$ , which rises linearly in  $r$  for small  $r$ . Following Ref. 12, the regularized velocity  $\mathbf{w}_v$  is decomposed into “incompressible” (divergence-free) and “compressible” (solenoidal) parts,  $\mathbf{w}_v = \mathbf{w}_i + \mathbf{w}_c$ , with  $\nabla \cdot \mathbf{w}_i = 0$ ,  $\nabla \times \mathbf{w}_c = 0$ , to distinguish vortical and rotationless motion of the fluid.

For comparison of the kinetic-energy spectrum with the single-particle spectra  $n(k)$ , we determine occupation numbers corresponding to the different energy fractions as  $n_\delta(k) = k^{-d-1} E_\delta(k)$ ,  $\delta \in \{i, c, q\}$ . The resulting spectra  $n_i(k)$ ,  $n_c(k)$ , and  $n_q(k)$  add up to the single-particle spectrum  $n(k) = n_i(k) + n_c(k) + n_q(k)$  discussed before. The components are shown separately, for  $d = 2$  and  $d = 3$ , in Figs. 4 and 5, respectively. Red circles denote  $n_i$ , filled blue squares show

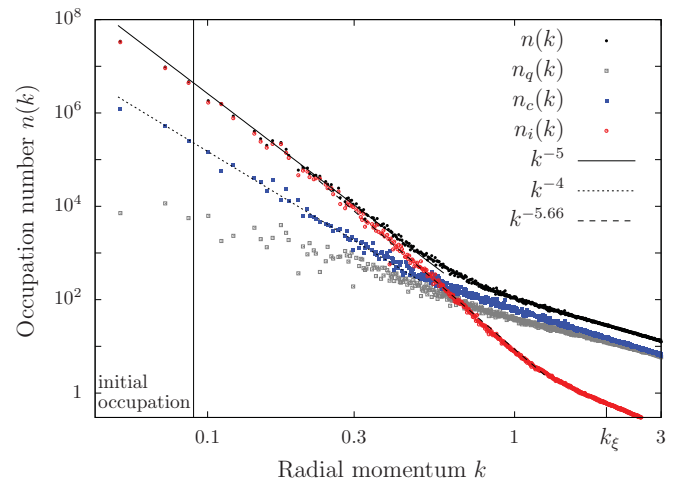


FIG. 5. (Color online) Same as in Fig. 4, for the run in  $d = 3$  dimensions shown in Fig. 2, at the time  $\bar{t} = 1640$  (lower right-hand panel).

the dependence of  $n_c$ , and open gray squares that of  $n_q$ . Qualitatively, the results are the same for  $d = 2$  and  $d = 3$ . Excitations with large wave numbers are thermally distributed. In this regime, the spectrum  $n(k) \sim k^{-2}$  is dominated by the compressible and quantum-pressure components. For smaller wave numbers the scaling changes to  $n(k) \sim k^{-d-2}$ , being dominated by the velocity  $\mathbf{w}_v$ . Moreover, we find that it is this decomposition into  $n_i$  and  $n_c$  which, for intermediate wave numbers, allows the incompressible part of the energy to develop a Kolmogorov-like scaling  $\sim k^{-5/3-d-1}$  above the scale  $k_l \sim 2\pi/l$  determined by the mean distance  $l$  between vortex cores. While the scaling of the sum of these components is predicted by the field-theoretic analysis in Ref. 6, a rising compressible part allows the incompressible contribution to deviate from the IR power law and to develop the observed scaling. Toward the IR limit, the compressible part becomes too weak such that the scaling of  $n_i$  goes over to  $\zeta = d + 2$ .

One can show that the analytically predicted infrared  $n(k) \sim k^{-4}$  in  $d = 2$  is consistent with a finite density of independent vortices and antivortices. The IR scaling  $\sim k^{-d-1}$  of the compressible component suggests an interpretation in terms of acoustic turbulence.<sup>17,19,22</sup> Our results show that this component survives for a limited period beyond the time when all vortical excitations have mutually annihilated. The observed scaling corroborates the numerical

findings of Ref. 23, whereby we refrain from sharing the interpretation of the power law.

In summary, our results show a distinct power-law behavior  $k^{-\zeta}$  of the single-particle momentum spectrum  $n(k)$  as well as of different components of the kinetic-energy distribution over the radial wave number  $k$ . Scaling exponents  $\zeta$  of  $n(k)$  corroborate the analytical predictions of Ref. 6. Our findings suggest that local field expectation values and short- to intermediate-range coherence, including topological excitations, are at the basis of the infrared power laws predicted within nonperturbative dynamical field theory.<sup>4-6</sup> For the chosen generic initial conditions, excitations on the top of this classical field background support an interpretation in terms of acoustic wave turbulence. The connection of these phenomena with *ab initio* dynamical field theoretic methods points a way to unified analytical studies of turbulence and gives hints how the proposed dynamical critical phenomena in relativistic systems<sup>4,5,7</sup> can be realized in nature.

T.G. and D.S. thank J. Berges and C. Scheppach for collaboration on related work. The authors thank C. Bodet, E. Calzetta, B. Eckhardt, L. Glazman, C. Gross, H. Horner, M. Kronenwett, M. K. Oberthaler, J. M. Pawłowski, M. Schmidt, J. Schole, and B. Svistunov for useful discussions, and Deutsche Forschungsgemeinschaft, University of Heidelberg (FRONTIER), and the Helmholtz Association (HA216/EMMI) for support.

\*t.gasenz@uni-heidelberg.de

<sup>1</sup>L. F. Richardson, *Proc. R. Soc. London A* **97**, 354 (1920); U. Frisch, *Turbulence* (Cambridge University Press, Cambridge, UK, 1995).

<sup>2</sup>A. N. Kolmogorov, *Proc. USSR Acad. Sci.* **30**, 299 (1941); *Proc. R. Soc. London A* **434**, 9 (1991).

<sup>3</sup>R. Micha and I. I. Tkachev, *Phys. Rev. Lett.* **90**, 121301 (2003).

<sup>4</sup>J. Berges, A. Rothkopf, and J. Schmidt, *Phys. Rev. Lett.* **101**, 041603 (2008).

<sup>5</sup>J. Berges and G. Hoffmeister, *Nucl. Phys. B* **813**, 383 (2009); J. Berges, S. Scheffler, and D. Sixty, *Phys. Lett. B* **681**, 362 (2009); J. Berges and D. Sixty, *Phys. Rev. D* **83**, 085004 (2011).

<sup>6</sup>C. Scheppach, J. Berges, and T. Gasenzer, *Phys. Rev. A* **81**, 033611 (2010).

<sup>7</sup>P. B. Arnold and G. D. Moore, *Phys. Rev. D* **73**, 025006 (2006); A. H. Mueller, A. I. Shoshi, and S. M. H. Wong, *Nucl. Phys. B* **760**, 145 (2007); M. E. Carrington and A. Rebhan, e-print arXiv:1011.0393.

<sup>8</sup>*Progress in Low Temperature Physics, Vol. 16: Quantum Turbulence*, edited by W. P. Halperin and M. Tsubota (Elsevier, Amsterdam, 2008); R. J. Donnelly, *Quantized Vortices in Liquid He II* (Cambridge University Press, Cambridge, UK, 1991).

<sup>9</sup>L. Onsager, *Nuovo Cimento Suppl.* **6**, 249 (1949).

<sup>10</sup>R. P. Feynman, in *Progress in Low Temperature Physics Vol. 1*, edited by C. J. Gorter (North-Holland, Amsterdam, 1955), p. 17.

<sup>11</sup>W. F. Vinen and J. J. Niemela, *J. Low Temp. Phys.* **128**, 167 (2002).

<sup>12</sup>C. Nore, M. Abid, and M. E. Brachet, *Phys. Rev. Lett.* **78**, 3896 (1997); *Phys. Fluids* **9**, 2644 (1997).

<sup>13</sup>T. Araki, M. Tsubota, and S. K. Nemirovskii, *Phys. Rev. Lett.* **89**, 145301 (2002); M. Kobayashi and M. Tsubota, *ibid.* **94**, 065302 (2005); T. Araki, M. Tsubota, and S. K. Nemirovskii, *J. Phys. Soc. Jpn.* **74**, 3248 (2005); M. Tsubota, K. Kasamatsu, and M. Kobayashi, e-print arXiv:1004.5458v2.

<sup>14</sup>T.-L. Horng, C. H. Hsueh, and S. C. Gou *Phys. Rev. A* **77**, 063625 (2008); T.-L. Horng, C. H. Hsueh, S. W. Su, Y. M. Kao, and S. C. Gou, *ibid.* **80**, 023618 (2009).

<sup>15</sup>V. I. Yukalov, *Laser Phys. Lett.* **7**, 467 (2010).

<sup>16</sup>C. J. Foster, P. B. Blakie, and M. J. Davis, *Phys. Rev. A* **81**, 023623 (2010).

<sup>17</sup>Y. Kagan, B. V. Svistunov, and G. V. Shlyapnikov, *Zh. Eksp. Teor. Fiz.* **101**, 528 (1992) [*Sov. Phys. JETP* **74**, 279]; Y. Kagan and B. V. Svistunov, *Zh. Eksp. Teor. Fiz.* **105**, 353 (1994); Y. Kagan, B. V. Svistunov, and G. V. Shlyapnikov, *Sov. Phys. JETP* **78**, 187.

<sup>18</sup>N. G. Berloff and B. V. Svistunov, *Phys. Rev. A* **66**, 013603 (2002).

<sup>19</sup>E. V. Kozik and B. V. Svistunov, *J. Low Temp. Phys.* **156**, 215 (2009).

<sup>20</sup>C. N. Weiler *et al.*, *Nature (London)* **455**, 454 (2008); T. W. Neely, E. C. Samson, A. S. Bradley, M. J. Davis, and B. P. Anderson, *Phys. Rev. Lett.* **104**, 160401 (2010).

<sup>21</sup>E. A. L. Henn *et al.*, *Phys. Rev. Lett.* **103**, 045301 (2009).

<sup>22</sup>V. E. Zakharov, V. S. L'vov, and G. Falkovich, *Kolmogorov Spectra of Turbulence I: Wave Turbulence* (Springer, Berlin, 1992).

<sup>23</sup>S. Khlebnikov, *Phys. Rev. A* **66**, 063606 (2002).